Journal of Microbiological Methods 108 (2015) 36–44

Contents lists available at ScienceDirect

Journal of Microbiological Methods

journal homepage: www.elsevier.com/locate/jmicmeth

Simulating distal gut mucosal and luminal communities using packed-column biofilm reactors and an in vitro chemostat model

Julie A.K. McDonald [a], Susana Fuentes [b], Kathleen Schroeter [a], Ineke Heikamp-deJong [b], Cezar M. Khursigara [a], Willem M. de Vos [b], Emma Allen-Vercoe [a,*]

[a] Department of Molecular and Cellular Biology, University of Guelph, 50 Stone Road East, Guelph, Ontario N1G 2W1, Canada
[b] Laboratory of Microbiology, Wageningen University, Wageningen, The Netherlands

ARTICLE INFO

Article history:
Received 6 October 2014
Received in revised form 17 November 2014
Accepted 17 November 2014
Available online 20 November 2014

Keywords:
Biofilm
Chemostat
DGGE
HITChip
Human gut microbiota
Microbial ecology

ABSTRACT

In vivo studies of human mucosal gut microbiota are often limited to end-point analyses and confounded by bowel cleansing procedures. Therefore, we used biofilm reactors to incorporate a simulated mucosal environment into an *in vitro* gut chemostat model. Communities developed were complex, reproducible, distinct, and representative of *in vivo* communities.

1. Introduction

The human intestine is colonized by a complex microbial community collectively referred to as the gut microbiota. The composition of the microbiota varies depending on the segment of the intestinal tract being sampled, with the most diverse community found in the distal gut (Sekirov et al., 2010; Backhed et al., 2005; Gaskins et al., 2008; Booijink et al., 2010). In addition to heterogeneity along the length of the intestinal tract, gut communities also vary within an intestinal segment (Sekirov et al., 2010). Previous literature has described distinct communities harbored in feces and mucosa (biopsy) (Zoetendal et al., 2002; Durban et al., 2011). Mucosal communities are thought to be particularly important to host health due to their proximity to the host epithelium (Sun et al., 2010).

The intestinal epithelium is separated from the gut lumen by a thick mucus layer (Sekirov et al., 2010). Community composition within this layer depends on a variety of factors, including the ability of microorganisms to bind to, degrade, and gain nutrients from mucins, as well as their ability to resist the actions of host antimicrobial peptides and to tolerate the relatively increased oxygen levels in this niche (Van den Abbeele et al., 2011). Microbial associations with host mucins may allow microorganisms to persist within the gut environment through the avoidance of washout as well as protection from the greater disturbances encountered by their luminal counterparts (Van den Abbeele et al., 2012b). These communities of microorganisms are able to do this by forming 'biofilm' structures, defined as matrix-enclosed microbial ecosystems that grow adherent to surfaces and/or to each other (Costerton et al., 1995).

While human mucosal communities have been characterized in vivo by analyzing microorganisms adherent to colonic biopsy specimens (Zoetendal et al., 2002; Durban et al., 2011), specimens collected via endoscopy are often limited to end-point analyses and studies may be confounded by the use of prior bowel cleansing procedures (Durban et al., 2011; Van den Abbeele et al., 2012b). Thus, dynamic monitoring of gut microbial communities is often conducted using fecal samples, which are not representative of mucosal community composition (Van den Abbeele et al., 2012b; Zoetendal et al., 2002).

In vitro models represent a useful alternative to in vivo biopsies for the study of mucosal communities (Van den Abbeele et al., 2009, 2012a,b; Vermeiren et al., 2012; Macfarlane et al., 2005; Probert and Gibson, 2004), however, such models would benefit from a more detailed characterization of planktonic and biofilm reproducibility, diversity, and response to perturbation. Van den Abbeele et al. (2012a,b) made several suggestions to improve upon these existing models, including: culturing biofilms from a distal colon vessel, coating scaffolds with mucin using an agar-independent method, harvesting the biofilms without disturbing planktonic and biofilm community stability, and harvesting the biofilms without opening the vessel and exposing the microbial cultures to oxygen (Van den Abbeele et al., 2012a). In a

* Corresponding author. Tel.: +1 519 824 4120x53366; fax: +1 519 837 1802.
E-mail address: eav@uoguelph.ca (E. Allen-Vercoe).

http://dx.doi.org/10.1016/j.mimet.2014.11.007
0167-7012/

previous study (McDonald et al., 2013) we described and validated a luminal-only in vitro gut model that allowed us to culture planktonic communities. In this study, we used packed-column biofilm reactors to incorporate a simulated mucosal environment into our twin-vessel single-stage chemostat model of the human distal gut, allowing us to simultaneously culture both planktonic and biofilm communities. Our aims were to determine whether planktonic and biofilm communities were (i) reproducible and stable over time, (ii) had distinct microbial compositions, and (iii) had varying responses to antibiotic perturbation.

2. Materials and methods

2.1. Inoculation, operation and sampling of single-stage chemostats

The Research Ethics Board of the University of Guelph approved this study (REB#09AP011). An Infors Multifors bioreactor system (Infors, Switzerland) was used for this work (McDonald et al., 2013). Chemostat inoculum and growth medium were prepared and vessels were inoculated and operated as previously described (McDonald et al., 2013). For this study, a fresh fecal sample was provided by a healthy 25 year-old female with no recent history of antibiotic treatment within 11 months prior to this study. Vessels 1 and 2 (referred to as V1 and V2, respectively) were inoculated with an identical fecal inoculum prepared from the donor stool. Vessels were operated using a medium feed rate of 400 mL/day to mimic a transit time of 24 h (Allison et al., 1989; Duncan et al., 2003). A stabilization period of 36 days without experimental manipulation was used to allow the communities to reach steady state (McDonald et al., 2013). The growth medium used for this study has been previously described (McDonald et al., 2013) and contained a mix of insoluble and soluble starches, vitamins, trace elements, and porcine gastric mucin, type II (4 g/L, Sigma-Aldrich, Oakville, Ontario). Cultures were gently agitated and sparged with O_2-free N_2, pH was set to 6.9–7.0, and vessels were allowed to run for 48 days post-inoculation. 4 mL was sampled daily from each chemostat vessel and archived at −80 °C.

2.2. Packed-column biofilm reactor preparation

A simulated mucosal environment was incorporated into our distal gut chemostat model using glass-jacketed distilling condenser columns (10 mm inner diameter, 280 mm length, 34 mL total volume) (Fig. 1) (Ferrera et al., 2004). Each column was packed with pieces of silicone tubing (HelixMark biomedical/pharmaceutical grade platinum-cured silicone tubing; approximately 2.5 mm width, 5 mm length) to provide a large surface for microbial attachment. Silicone was chosen as an agar-independent substrate for biofilm growth because of its mucin-binding capabilities and autoclavability (unpublished observations; (Shi et al., 2000). An independent peristaltic pump fitted with silicone tubing (VWR; Mississauga, Ontario) was used to circulate culture from the vessel, through the packed column (maintained at 37 °C using a circulating water bath), and back in to the vessel at a flow rate matching the parent vessel. Two packed-column reactors were attached to each vessel throughout the course of the experiment (Fig. 2) according to the following schedule: 'B1' days 0–36; 'B2' days 0–41; 'B3' days 36–48; and 'B4' days 41–48. This schedule was set up in order to maximize experimental endpoints while still allowing mature biofilm formation, taking into account the time needed for the vessels to attain steady-state conditions, as previously described (McDonald et al., 2013).

2.3. Biofilm harvest

To harvest biofilms from the packed-column reactors, 25 mL of sterile phosphate buffered saline (PBS, Gibco, Life Technologies Corporation; Grand Island, New York) was allowed to flush through the column by gravity feed (to wash away non-adherent microorganisms), and then column packing material was transferred to a sterile conical tube, diluted in 15 mL of Tris EDTA (TE, pH 8.0) and placed in a sonicating water bath for 3 min (Branson; Shelton, Connecticut) (Sanchez et al., 2008). Following sonication the biofilm became suspended in the TE buffer and the suspension was transferred into another sterile conical tube. The biofilm-TE mixture was gently pipetted several times to fully homogenize the biofilm, and the suspension was aliquoted and stored at −80 °C.

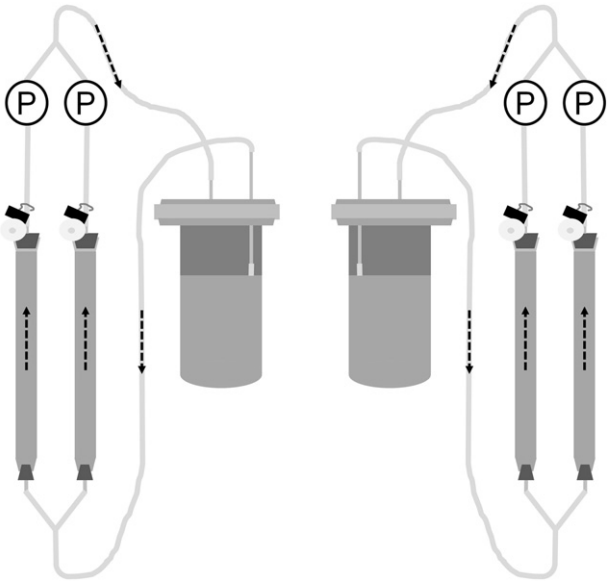

Fig. 1. Packed-column biofilm reactor set-up illustrating the attachment of tubing to the columns and vessel. P represents the location of the peristaltic pumps and the dashed arrows illustrate the direction of culture circulation.

2.4. Clindamycin-induced perturbation

Clindamycin (clindamycin 2-phosphate, Sigma-Aldrich) was directly added to steady state V1 (test vessel) according to a physiologically relevant regime (simulating a typical clinical course of this antibiotic and its pharmacological accumulation in stool) (Kager et al., 1981). Clindamycin was administered to V1 twice daily, with dosages 12 h apart: day 36 (of chemostat run) = 12.6 μg/mL, day 37 = 16.6 μg/mL, day 38 = 22.4 μg/mL, day 39 = 124.7 μg/mL, day 40 = 203.8 μg/mL. Equal dosage volumes of sterile water were added to V2 (control, untreated vessel).

2.5. DNA extraction

DNA was extracted from archived samples using a previously described method (McDonald et al., 2013) involving a combination of bead beating, inhibitor removal (Omega Bio-Tek E.Z.N.A.® Stool DNA kit (Norcross, Georgia)) and magnetic-bead-based gDNA purification (Maxwell®16 DNA Purification Kit (Promega; Madison, Wisconsin)).

2.6. Denaturing gradient gel electrophoresis (DGGE) analysis

DNA was extracted from planktonic communities from both vessels every two days starting on day 0 (immediately following inoculation) until the end of the experiment (day 48). DGGE was used as a high throughput molecular fingerprinting technique to monitor changes in the overall structure of the planktonic communities, and to indicate appropriate samples for HITChip analysis. Sample 16S rRNA genes (V3 region) were amplified using primers HDA1 and HDA2-GC (Tannock et al., 2000), and separated using the DCode system (Bio-Rad Laboratories, Hercules, California) using the method of Muyzer et al. (1993), with small modifications as described previously (McDonald et al., 2013).

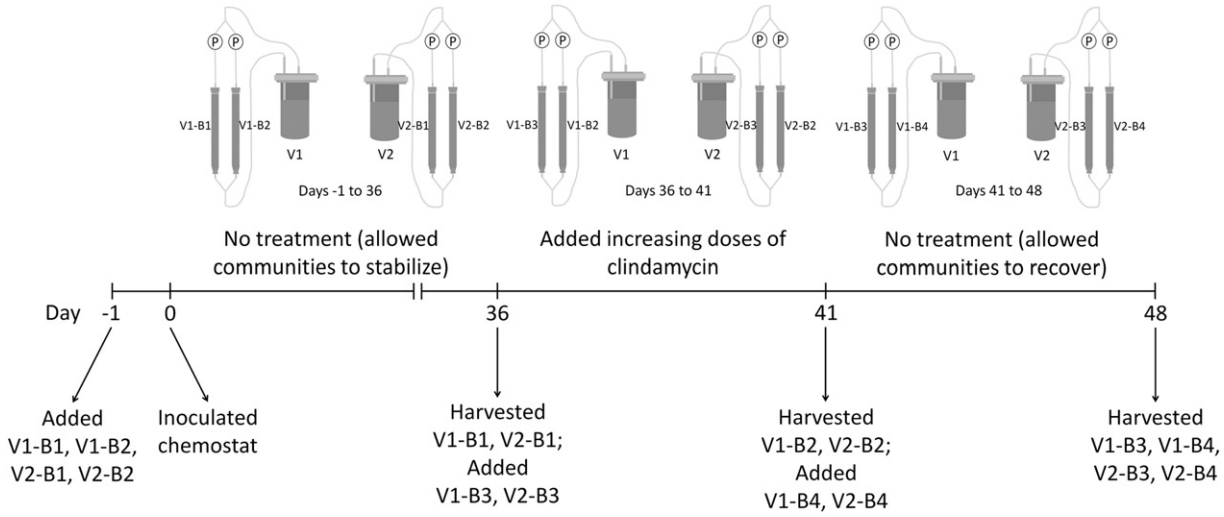

Fig. 2. Experimental design outlining in which packed column biofilm reactors were attached to each vessel at different points of the experiment. Biofilm samples cultured from V1 or V2 between days 0 and 36 are referred to as V1-B1 or V2-B1 (not exposed to clindamycin). Biofilm samples cultured from V1 or V2 between days 0 and 41 are referred to as V1-B2 (exposed to clindamycin between days 36 and 41) or V2-B2 (exposed to water between days 36 and 41). Biofilm samples cultured from V1 or V2 between days 36 and 48 are referred to as V1-B3 (exposed to clindamycin between days 36 and 41) or V2-B3 (exposed to water between days 36 and 41). Biofilm samples cultured from V1 or V2 between days 41 and 48 are referred to as V1-B4 (growth initiated following the clindamycin treatment period) or V2-B4 (growth initiated following the water addition period).

Images were captured using a SynGene G-Box gel documentation system and processed using GeneSnap software (version 6.08.04, Synoptics Ltd; Cambridge, UK), normalized for saturation, and then analyzed using Syngene GeneTools software (version 4.01.03, Synoptics Ltd). Similarity matrices and dendrograms were generated using an unweighted pair group with mathematical averages (UPGMA) and the Pearson coefficient of similarity. Similarity indices and correlation coefficients were calculated as previously described (McDonald et al., 2013), as were gel-specific vessel comparison "cut-off thresholds" which allowed for evaluation of gel-generated error. Samples with correlation coefficients greater than the cut-off threshold were considered identical, and samples were considered similar if the correlation coefficient values were within 5% of the cut-off value.

2.7. Community dynamics

Community dynamics were measured by running DGGE gels and using them to calculate rate-of-change (Δt) values. Δt values were calculated by averaging the change between consecutive DGGE profiles of the same community over two day intervals, where %change = 100 − %similarity, as previously described (Possemiers et al., 2004; Marzorati et al., 2008). Δt values were used to create moving window correlation plots that allowed for the assessment of ecosystem stability. Rate-of-change cut-off thresholds were calculated by subtracting vessel comparison cut-off threshold values from 100%.

2.8. Phylogenetic microarray (HITChip) analysis

Microbial community composition of 15 key samples (1 fecal inoculum sample, 6 planktonic community samples (V1 days 36, 41, 48 and V2 days 36, 41, 48), and 8 biofilm community samples (V1-B1, V1-B2, V1-B3, V1-B4, V2-B1, V2-B2, V2-B3, V2-B4) were evaluated using the Human Intestinal Tract Chip (HITChip), a phylogenetic microarray that contains over 5000 probes based on 16S rRNA gene sequences of over 1100 intestinal bacterial phylotypes (Rajilic-Stojanovic et al., 2009). HITChip analyses were performed as previously described (McDonald et al., 2013) using standard protocols (Jalanka-Tuovinen et al., 2011).

2.9. Shannon diversity index, Shannon equitability index, richness

The Shannon diversity index (H′) was calculated according to previous studies (Magurran, 2004; Gafan et al., 2005). Briefly:

$$H' = -\sum_{i=1}^{S}(p_i)(\ln p_i)$$

where, for DGGE profiles, S represented the total number of DGGE bands and p_i represented the proportion of the ith band (band peak height) (Gafan et al., 2005; Girvan et al., 2005; Duarte et al., 2012). For HITChip data, S represented the total number of hybridized probe sequences and p_i represented the proportion of the ith hybridized probe sequence (hybridization signal intensity). The Shannon equitability index ($E_{H'}$) was calculated as follows (Pielou, 1975; Smith and Wilson, 1996; Girvan et al., 2005): $E_{H'} = H' / \ln S$. Ecosystem richness (S) was approximated by enumerating the total number of bands present in a given DGGE profile or the total number of hybridized probe sequences for HITChip data (Fromin et al., 2002; Gafan et al., 2005; Girvan et al., 2005; Rajilic-Stojanovic et al., 2009). DGGE H′, $E_{H'}$ and S values plotted over time were adjusted to illustrate general patterns of ecological change over the course of a run as described previously (McDonald et al., 2013).

3. Results

3.1. Planktonic communities were reproducible and stable over time

Comparison of the microbiota of planktonic community samples (V1-P and V2-P) from the two vessels by DGGE showed that these communities were reproducible over time, (correlation coefficient values were above the gel-defined cut-off thresholds immediately following inoculation until day 36) (Fig. 3a). Although higher Δt values were seen at earlier time points, these values decreased and stabilized in both vessels as the communities reached steady state (days 34–36) (Fig. 3b). H′, $E_{H'}$, and S values were reproducible for V1-P and V2-P communities between days 0 and 36 and stabilized upon the establishment of steady state conditions (Fig. 3c, d, e).

Principal component analysis (PCA) of HITChip data provided an overview of how key samples clustered together based on their genus-like level compositions (Fig. 4, Table 1). V1-P and V2-P communities clustered together at steady state and V2-P communities (control

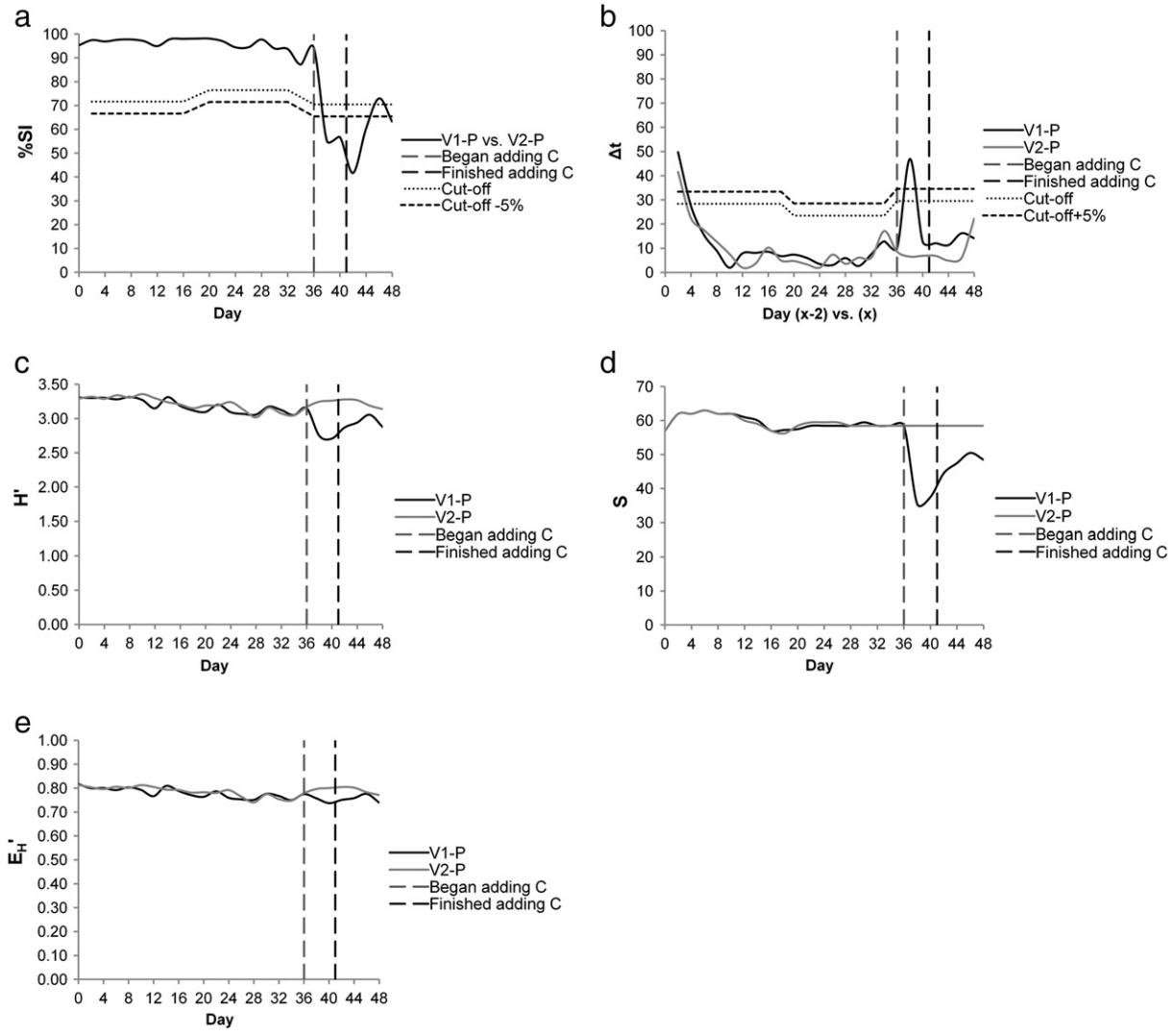

Fig. 3. DGGE analysis of the planktonic communities from two chemostat vessels (V1-P and V2-P) modeling the human distal gut prior to, during, and following a clindamycin (C) treatment period. a) Correlation coefficients (expressed as percentages) comparing the profiles of each vessel at identical time points. b) Community dynamics calculated using moving window correlation analysis as previously described (Possemiers et al., 2004; Marzorati et al., 2008). c) Adjusted Shannon diversity index (H′). d) Adjusted band richness (S). e) Adjusted Shannon equitability index (E_H′).

vessel) had similar compositions over the course of the experiment (on days 36, 41, and 48).

3.2. Biofilm growth was reproducible

Cultured biofilm community samples (on day 36 = V1-B1 and V2-B1) analyzed by HITChip clustered together by PCA and indicated that the biofilm communities from each vessel were compositionally similar (Fig. 4, Table 1) and were reproducible (Tables S1 and S2). Photographs of V1-B1 and V1-B2 biofilms also revealed gross biofilm morphology reproducibility at steady state (Fig. S1). V2 biofilm communities followed the same trend and were phylogenetically similar in composition (Fig. 4). Although V1-B1 and V2-B1 biofilm formation was reproducible over time, Pearson's similarity values were slightly higher when biofilm initiation, harvest, and development times were more similar (Table S1).

3.3. Planktonic and biofilm communities had distinct community compositions

PCA of HITChip data showed that planktonic and biofilm communities originating from the same vessel clustered separately from each other (Fig. 4), and this was confirmed by HITChip correlation coefficients (Table S1). HITChip indicated that biofilm samples contained more Firmicutes (particularly *Clostridium* cluster IV), and less Bacteroidetes compared to the corresponding steady state planktonic communities (Table 2). Verrucomicrobia was increased in the biofilm communities compared to the planktonic communities, reflecting the mucus location of this unique group of bacteria, represented by *Akkermansia muciniphila* (Belzer and de Vos, 2012).

3.4. Clindamycin treatment caused a shift in planktonic community composition

Comparison of V1-P and V2-P communities to each other across the antibiotic treatment period showed twin-vessel correlation coefficients decreased during antibiotic treatment, and increased once antibiotic addition was stopped (Fig. 3a). However, community similarity did not recover to pre-clindamycin levels by the end of the experiment. V1-P, H′, E_H′, and *S* values decreased during the treatment period and began to increase once clindamycin addition was stopped (Fig. 3c,d,e, Table S2), but did not return to baseline values by the end of the experiment. Δt values peaked between days 36 and 38 indicating that the bulk of clindamycin-associated compositional change took place early on

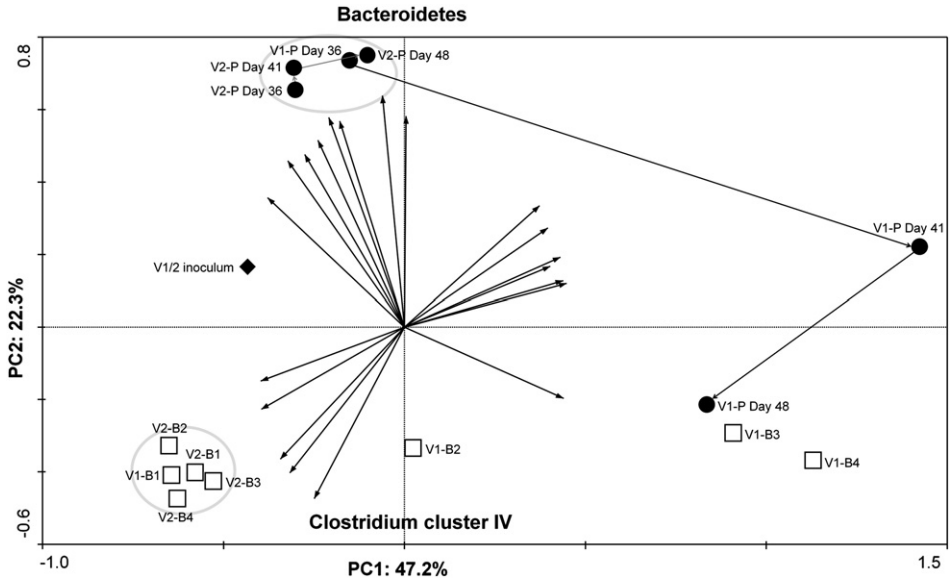

Fig. 4. Principal component analysis (PCA) at the genus-like level based on HITChip data of the fecal inoculum (◆), planktonic communities (●), and biofilm communities (□). Arrows indicate shifts in planktonic samples following clindamycin or water treatment. Light gray circles indicate clustering of planktonic or biofilm samples not exposed to clindamycin.

during the dosing regimen (Fig. 3b). Although Δt values for both communities were stable following clindamycin treatment, V1 Δt was generally higher than V2 Δt (indicating that planktonic communities in V1 were still in flux).

PCA of HITChip data showed that V1-P communities sampled after clindamycin exposure clustered separately from untreated planktonic samples (Fig. 4); an increased level of several *Bacteroides* spp. and bacteria related to *Subdoligranulum variabile* and *Escherichia coli*, and a decreased level of Firmicutes (especially groups belonging to *Clostridium* clusters IV and XIVa) and some members of the Bacteroidetes (Table S3, day 41) were seen compared to control planktonic communities. By day 48, during the clindamycin wash-out period, members of the V1-P community, particularly *Bacteroides* spp., showed some recovery. Verrucomicrobia (represented by *A. muciniphila)* abundance decreased during antibiotic treatment and began to increase once antibiotic treatment was stopped. Interestingly, levels of bacteria related to *Clostridium orbiscindens* showed a 'rebound' effect, where its abundance was decreased immediately following antibiotic treatment but grew beyond baseline levels during the washout/recovery period. Bacteria related to *S. variabile* were greatly reduced during the recovery period, whereas bacteria related to *Dorea formicigenerans* appeared to be resistant to clindamycin treatment and were able to grow beyond baseline levels after the antibiotic treatment

Table 1
Percent abundance of higher taxonomic groups (~ phylum/class level) based on HITChip analysis for the fecal inoculum (fecal inoc), planktonic communities (V1-P and V2-P) and biofilm communities (V1-B and V2-B).

Higher taxonomic groups		Fecal inoc	V1-P day 36	V2-P day 36	V1-P day 41	V2-P day 41	V1-P day 48	V2-P day 48	V1-B1	V2-B1	V1-B2	V2-B2	V1-B3	V2-B3	V1-B4	V2-B4
	Actinobacteria	0.45	0.36	0.52	0.73	0.44	0.50	0.54	1.50	1.08	2.52	1.86	0.56	0.50	0.54	0.43
	Bacteroidetes	21.69	50.01	45.49	63.61	49.15	36.43	47.63	18.72	19.55	27.03	20.70	38.86	22.58	48.68	19.15
Firmicutes	Bacilli	0.79	0.65	0.94	1.23	0.77	0.87	0.95	0.79	0.69	1.01	0.87	0.91	0.79	0.93	0.74
	Clostridium cluster I	0.18	0.20	0.29	0.39	0.24	0.26	0.30	0.29	0.32	0.40	0.35	0.28	0.26	0.29	0.24
	Clostridium cluster III	0.15	0.09	0.14	0.13	0.14	0.11	0.13	0.14	0.25	0.22	0.26	0.19	0.43	0.12	0.37
	Clostridium cluster IV	31.01	14.90	15.20	18.45	18.84	29.25	12.24	30.46	35.26	28.21	30.16	31.95	26.06	21.62	31.11
	Clostridium cluster IX	1.26	0.31	0.46	0.53	0.38	0.39	0.46	0.46	0.39	0.54	0.52	0.43	0.46	0.41	0.46
	Clostridium cluster XI	1.31	0.27	0.37	0.44	0.31	0.31	0.36	0.45	0.38	0.71	0.65	0.32	0.27	0.32	0.25
	Clostridium cluster XIII	0.03	0.04	0.05	0.08	0.04	0.05	0.06	0.04	0.04	0.06	0.05	0.05	0.04	0.05	0.04
	Clostridium cluster XIVa	39.26	28.86	30.83	9.53	25.06	27.66	22.93	36.01	32.32	29.63	32.62	21.05	30.84	13.92	29.97
	Clostridium cluster XV	0.03	0.03	0.05	0.08	0.04	0.05	0.05	0.04	0.04	0.05	0.04	0.05	0.04	0.05	0.04
	Clostridium cluster XVI	0.11	0.11	0.16	0.23	0.13	0.16	0.16	0.13	0.12	0.17	0.15	0.16	0.14	0.16	0.13
	Clostridium cluster XVII	0.02	0.03	0.04	0.06	0.04	0.04	0.05	0.04	0.03	0.05	0.04	0.05	0.04	0.05	0.03
	Clostridium cluster XVIII	0.07	0.08	0.11	0.47	0.09	0.10	0.11	0.10	0.07	0.14	0.10	0.14	0.09	0.15	0.08
	Uncultured *Clostridiales*	1.67	0.79	1.06	1.01	0.71	0.75	10.19	1.45	1.17	1.68	1.41	1.22	1.53	0.73	1.79
	Total Firmicutes	75.90	46.36	49.69	32.63	46.78	60.00	47.97	70.40	71.09	62.85	67.23	56.79	61.00	38.81	65.26
	Cyanobacteria	0.01	0.01	0.01	0.01	0.01	0.01	0.01	0.01	0.01	0.01	0.01	0.01	0.01	0.01	0.01
	Fusobacteria	0.05	0.07	0.10	0.14	0.08	0.09	0.10	0.08	0.07	0.10	0.09	0.10	0.08	0.10	0.07
	Proteobacteria	0.69	1.41	1.93	2.49	1.68	1.79	1.86	5.37	5.34	3.17	4.35	2.94	11.30	11.35	8.45
	Spirochaetes	0.01	0.01	0.02	0.03	0.02	0.02	0.02	0.02	0.01	0.02	0.02	0.02	0.02	0.02	0.02
Tenericutes	Asteroleplasma	0.01	0.01	0.01	0.02	0.01	0.01	0.01	0.01	0.01	0.01	0.01	0.01	0.01	0.01	0.01
	Uncultured Mollicutes	0.08	0.11	0.16	0.21	0.13	0.15	0.16	0.12	0.11	0.16	0.14	0.15	0.13	0.16	0.11
	Verrucomicrobia	1.11	1.66	2.07	0.13	1.72	0.99	1.70	3.77	2.73	4.11	5.61	0.57	4.39	0.31	6.50

Table 2
Genus-like level bacterial groups significantly different (p = 0.02, q = 0.05) between average planktonic communities and average biofilm communities for samples not exposed to clindamycin treatment. P values were calculated using the Wilcoxon signed-rank test corrected for multiple comparisons. The fold changes (biofilm/planktonic samples) shown in green are >2.5 (higher in biofilm samples) and shown in red are <0.5 (lower in biofilm samples). SD = standard deviation.

Level 1 (~ phylum/class level)	Level 2 (genus-like level)	Planktonic abundance (%)	SD	Biofilm abundance (%)	SD	Fold change (biofilm/planktonic)
Bacteroidetes	*Alistipes et rel.*	1.14	0.20	0.63	0.06	0.55
	Bacteroides fragilis et rel.	5.25	0.94	1.61	0.27	0.31
	Bacteroides ovatus et rel.	7.52	1.52	1.93	0.41	0.26
	Bacteroides plebeius et rel.	0.93	0.14	0.58	0.09	0.62
	Bacteroides splachnicus et rel.	0.59	0.07	0.40	0.03	0.68
	Bacteroides stercoris et rel.	0.92	0.17	0.52	0.07	0.57
	Bacteroides vulgatus et rel.	19.71	2.62	7.85	1.27	0.40
	Prevotella melaninogenica et rel.	0.66	0.26	0.27	0.04	0.41
	Prevotella oralis et rel.	0.56	0.16	0.24	0.03	0.43
	Prevotella ruminicola et rel.	0.06	0.01	0.05	0.00	0.73
	Prevotella tannerae et rel.	0.50	0.04	0.26	0.02	0.52
	Tannerella et rel.	0.54	0.06	0.34	0.03	0.63
Bacilli	*Streptococcus mitis et rel.*	0.08	0.01	0.11	0.01	1.37
Clostridium cluster III	*Clostridium stercorarium et rel.*	0.12	0.02	0.28	0.11	2.43
Clostridium cluster IV	*Anaerotruncus colihominis et rel.*	0.27	0.03	0.69	0.12	2.50
	Clostridium cellulosi et rel.	0.84	0.18	2.49	0.30	2.96
	Clostridium leptum et rel.	1.81	0.48	3.13	0.29	1.73
	Clostridium orbiscindens et rel.	2.06	0.33	7.88	1.65	3.84
	Oscillospira guillermondii et rel.	4.96	1.47	12.49	1.28	2.52
	Ruminococcus bromii et rel.	2.79	0.61	0.51	0.06	0.18
	Subdoligranulum variable at rel.	0.79	0.04	1.08	0.29	1.37
Clostridium cluster IX	*Dialister*	0.12	0.02	0.19	0.02	1.62
Clostridium cluster XIVa	*Anaerostipes caccae et rel.*	0.29	0.03	0.42	0.07	1.43
	Clostridium sphenoides et rel.	2.45	0.22	1.79	0.24	0.73
	Clostridium symbiosum et rel.	19.28	3.11	25.67	1.87	1.33
	Lachnobacillus bovis et rel.	0.28	0.08	0.16	0.02	0.56
	Lachnospira pectinoschiza et rel.	0.22	0.03	0.33	0.03	1.46
	Ruminococcus obeum et rel.	1.07	0.07	0.89	0.06	0.83
Proteobacteria	*Burkholderia*	0.05	0.01	0.02	0.00	0.49
	Enterobacter aerogenes et rel.	0.21	0.03	0.13	0.01	0.61
	Escherichia coli et rel.	0.27	0.07	5.78	2.84	21.42
	Klebisiella pneumoniae et rel.	0.09	0.01	0.12	0.02	1.32
	Oceanospirillum	0.05	0.01	0.04	0.00	0.73
	Oxalobacter formigenes et rel.	0.20	0.04	0.11	0.01	0.56
	Serratia	0.01	0.00	0.09	0.03	6.66
	Sutterella wadsworthia et rel.	0.22	0.02	0.14	0.02	0.63
	Xanthomonadaceae	0.08	0.01	0.05	0.01	0.55
Verrucomicrobia	*Akkermansia*	1.79	0.19	4.60	1.49	2.57

was stopped. By day 48, members of *Clostridium* cluster XIVa that had been negatively affected by antibiotic treatment generally recovered to baseline abundances.

3.5. Clindamycin treatment altered the structure of simulated mucosal biofilms

Biofilm community perturbation following clindamycin exposure was compared both within reactors associated with a single vessel, as well as across reactors associated with a duplicate vessel. The gross morphologies of the biofilms are shown in Fig. S1; less biofilm growth for the clindamycin-treated vessel was seen. In general, H′, E_H′, and *S* values from biofilm samples decreased following clindamycin exposure (Table S2).

PCA of HITChip data showed that antibiotic-exposed biofilm communities clustered apart from unexposed biofilm communities (Fig. 4). V1-B3 and V1-B4 communities clustered more closely with the V1-P community at day 48 than with other biofilm communities, and the V1-B2 community was positioned between the clusters of control (unexposed) biofilm communities and the cluster of V1-B3, V1-B4, and V1-P day 48.

HITChip analysis indicated that despite exposure to clindamycin the V1-B2 biofilm was compositionally similar to unexposed biofilms (Table S4). Where differences were seen, the antibiotic treated vessel showed increased levels of *Bifidobacterium* spp. and bacteria related to *Bacteroides fragilis* and *Bacteroides ovatus*, and decreased levels of bacteria related to *Bacteroides plebeius*, *Bacteroides uniformis*, and *E. coli*. In general, Firmicutes members associated with biofilm samples were less affected by antibiotic perturbation than the corresponding planktonic samples.

Biofilm communities grown during and after clindamycin exposure (V1-B3 and V1-B4, respectively) were comparable, except that V1-B4 showed less similarity to control biofilms than V1-B3. Both V1-B3 and V1-B4 communities contained increased levels of bacteria related

to *B. fragilis*, *B. ovatus*, *Parabacteroides distasonis*, *S. variable* and *D. formicigenerans* and reduced levels of some members of the Bacteroidetes and Firmicutes compared to unexposed, control biofilm communities.

4. Discussion

Applying strategies to encourage physiologically relevant biofilm growth could improve in vitro models and create a more biologically relevant environment for the development of microbial ecosystems (Van den Abbeele et al., 2012a). In this study we characterized simulated luminal and mucosal distal gut communities in a twin-vessel single-stage chemostat model system that included a parallel packed-column biofilm reactor. The packed-column reactors we describe in this study used mucin-primed silicone to promote establishment of biofilms in the reactor, and at the same time provided a constant supply of mucin in the medium feed to sustain such biofilms. Unlike the gut epithelium, silicone is a non-shedding material, thus there are several limitations in physiological relevance for our study. Nevertheless, this work represents an advance on previous studies by allowing long-term modeling of the distal gut ecosystem with regular sampling, at the same time avoiding compromise of the ecosystem through opening of the vessel (with concurrent exposure to oxygen) (Macfarlane et al., 2005; Van den Abbeele et al., 2012a). In addition, priming and then feeding the system with mucin, as opposed to the use of e.g. agar substrates to immobilize mucin within the system (where the agar itself could influence ecosystem composition) represent an effective and cost-effective way to encourage biofilm growth in vitro (Macfarlane et al., 2005).

When bacterial phyla and classes are considered, in vivo studies have found an enrichment of Firmicutes (especially *Clostridium* cluster XIVa) over Bacteroidetes in human biopsy specimens (compared to fecal samples) (Eckburg et al., 2005; Frank et al., 2007; Hong et al., 2011; Shen et al., 2010; Wang et al., 2010; Willing et al., 2010). In agreement with this, HITChip analysis of our model system showed that biofilm samples contained more Firmicutes (especially *Clostridium* cluster IV), and less Bacteroidetes compared to steady state planktonic communities. Other biofilm-enriched models of the human distal gut have collectively shown that Bacteroidetes, Proteobacteria and *Bifidobacterium* spp. were enriched in the planktonic phase, whereas Firmicutes (especially *Clostridium* cluster XIVa), members of the *B. fragilis* group, *Enterobacterium* spp., and *Clostridium* spp. were enriched in the biofilm phase (Macfarlane et al., 2005; Van den Abbeele et al., 2012a). Variations in the composition of biofilm communities developed in our model relative to previous studies could be due to many factors, including differences in the composition of the fecal inoculum, the type of gut model employed (e.g. single-stage vs. multistage), the device used to culture biofilms (e.g. packed-column reactor vs. microcosms in a netted bag vs. gels in glass tubes), the growth medium composition, or the analysis techniques (e.g. HITChip vs. culturing). Further metabolomic analysis of samples obtained from in vitro supported gut microbial communities will help to further elucidate the extent to which our model can mimic the in vivo niche.

Previous gut models culturing planktonic communities were not able to culture *A. muciniphila* to high densities (Van den Abbeele et al., 2012a), presumably because *A. muciniphilia* is a mucus-colonizing bacterium shown to be present in higher abundance in healthy mucosa (Derrien et al., 2004; Swidsinski et al., 2011; Png et al., 2010). In our distal gut model we were able to culture *A. muciniphila* in both planktonic and biofilm communities (Table 1), with enrichment (>2.5 times higher) in the biofilm phase (Table 2), indicating the validity of our model.

Previous work has shown that planktonic communities developed in models of the luminal gut are reproducible, however the reproducibility of planktonic and biofilm communities in gut models that incorporate a simulated mucosal environment still requires validation (Van den Abbeele et al., 2010). To our knowledge, this is the first study indicating the reproducibility of simulated mucosal biofilms developed in a gut chemostat model. We found that planktonic communities from twin vessels were stable and had similar compositions by 34–36 days post-inoculation (Fig. 3), and that simulated mucosal biofilm composition was reproducible both within the same vessel system, as well as between independent systems run under identical conditions. Although we did not harvest biofilm samples at early time points during our runs, this remains a goal for future experiments, and should allow a more dynamic view of biofilm formation.

Clindamycin-induced perturbation of planktonic chemostat communities caused shifts in community structure that were consistent with changes previously observed in vivo. For example, HITChip analysis indicated an overall reduction of the Bacteroidetes and Firmicutes (especially groups belonging to *Clostridium* clusters IV and XIVa), and there was also an increase in the abundance of generally clindamycin-resistant Bacteriodetes (bacteria related to *B. fragilis* (Oteo et al., 2000) and *B. ovatus* (Smith, 1985)) as well as bacteria belonging to *E. coli* (Nyberg et al., 2007), and *S. variabile* (Table S5). Recovery of the abundance of these groups following a wash out period was incomplete. In vivo, the effect of clindamycin administration on the structure of fecal communities has been measured in humans and animal models. Kager et al. (1981) found that colorectal surgery patients receiving clindamycin prophylaxis had decreased fecal populations of anaerobic (including *Bacteroides* spp., *Clostridium* spp. and *Bifidobacterium* spp.) and aerobic (*Enterococcus* spp. and *Streptococcus* spp.) bacteria that recovered following antibiotic withdrawal (Kager et al., 1981). Using a more sensitive assay, Jernberg et al. (2007) found that clindamycin treatment caused a significant, sharp decline in *Bacteroides* diversity, which did not fully recover after treatment was withdrawn. In addition, this latter study indicated the persistence of clindamycin-resistant *Bacteroides* spp. (Jernberg et al., 2007). In mouse and hamster models, exposure to clindamycin resulted in a general reduction of fecal microbiota diversity although once again clindamycin-resistant microbes, including some members of the *Proteobacteria,* increased in abundance (Peterfreund et al., 2012; Reeves et al., 2011; Buffie et al., 2012). These results collectively support the relevance of our model (Fig. S2).

In this study, we show that clindamycin treatment altered the composition of simulated mucosal biofilms, and that the impact of clindamycin exposure was least when mature biofilms were exposed to the drug (V1-B2), and greatest when biofilms formed following clindamycin exposure (V1-B4). Although this has not been specifically modeled in chemostats supporting complex fecal communities until now, our finding is consistent with classical pure-culture chemostat studies of *Pseudomonas aeruginosa*; here it was demonstrated that established, older biofilm communities are more resistant to antibiotic perturbation than planktonic cells (Anwar et al., 1992; Anwar et al., 1989). In our study, the precise origin of the V1-B3 biofilm (which formed during the clindamycin exposure) was not determined; it could have been formed early during antibiotic treatment (bacteria can bind to mucin within 15 min) (Freter et al., 1981b; Freter et al., 1981a), or may have been seeded from sloughed off biofilm cells from other reactors attached to the system. Either of these scenarios would select for greater antibiotic resistance than in planktonic communities. Further analysis of biofilm biogenesis within our model system is warranted to help answer these questions and perhaps indicate biofilm cycling in vivo.

Validation of our model against in vivo studies that investigate the impact of antibiotic exposure on healthy gut mucosal communities is difficult, because few such studies have been carried out to date. However, Peterfreund et al. (2012) found that hamsters sensitized to *Clostridium difficile* infection using clindamycin demonstrated a loss of distinction between cecal luminal contents and tissue-associated communities (Peterfreund et al., 2012). This finding is consistent with our study where we show that biofilms that formed either during or following clindamycin exposure were more similar to their respective

recovering planktonic communities than to biofilms not exposed to antibiotics.

While we were able to demonstrate reproducibility of the model, we were limited by the amount of fecal inoculum material obtained in a single donation. Although in our previous work (McDonald et al., 2013) we have shown that planktonic chemostat communities seeded from the same donor using temporally separated donations tend towards a compositionally similar steady state, future work should address the effects of variability in fecal inocula on obtained biofilms. Using a single inoculum source donation, once at steady state the obtained planktonic and biofilm communities exhibited temporal stability, and showed distinct microbial compositions, which were perturbed to different degrees following antibiotic treatment.

In conclusion, we were able to successfully incorporate a simulated mucosal environment into our twin-vessel single-stage chemostat model of the human distal gut, and we suggest that this model can be effectively used in controlled experiments to more completely investigate the effect of perturbations on the luminal as well as the mucosal gut microbial ecosystem. In the light of recent studies indicating the importance of the gut microbiota in antibiotic-promoted diseases such as *C. difficile* infection (CDI), the availability of a relevant in vitro model will allow us to develop a model of CDI to test different therapeutic strategies before animal studies or human trials (Petrof et al., 2013a,b; Allen-Vercoe and Petrof, 2013; Lawley et al., 2012).

Supplementary data to this article can be found online at http://dx.doi.org/10.1016/j.mimet.2014.11.007.

Acknowledgments

This work was supported by the Canadian Institutes of Health Research Catalyst: Human Microbiome Award granted to EAV and the Ontario Ministry of Agriculture, Food and Rural Affairs (OMAFRA) (200216)/University of Guelph Partnership Grant (Food for Health) jointly awarded to EAV and CMK; and the Netherlands Organization for Scientific Research (Spinoza and Gravity) awarded to WMdV.

We thank Michelle Daigneault, Kaitlyn Oliphant, and Christian Ambrose for their technical assistance.

References

Allen-Vercoe, E., Petrof, E.O., 2013. Artificial stool transplantation: progress towards a safer, more effective and acceptable alternative. Expert Rev. Gastroenterol. Hepatol. 7, 291–293.

Allison, C., McFarlan, C., MacFarlane, G.T., 1989. Studies on mixed populations of human intestinal bacteria grown in single-stage and multistage continuous culture systems. Appl. Environ. Microbiol. 55, 672–678.

Anwar, H., van Biesen, T., Dasgupta, M., Lam, K., Costerton, J.W., 1989. Interaction of biofilm bacteria with antibiotics in a novel in vitro chemostat system. Antimicrob. Agents Chemother. 33, 1824–1826.

Anwar, H., Strap, J.L., Chen, K., Costerton, J.W., 1992. Dynamic interactions of biofilms of mucoid Pseudomonas aeruginosa with tobramycin and piperacillin. Antimicrob. Agents Chemother. 36, 1208–1214.

Backhed, F., Ley, R.E., Sonnenburg, J.L., Peterson, D.A., Gordon, J.I., 2005. Host-bacterial mutualism in the human intestine. Science 307, 1915–1920.

Belzer, C., de Vos, W.M., 2012. Microbes inside—from diversity to function: the case of *Akkermansia*. ISME J. 6, 1449–1458.

Booijink, C.C., El-Aidy, S., Rajilic-Stojanovic, M., Heilig, H.G., Troost, F.J., Smidt, H., et al., 2010. High temporal and inter-individual variation detected in the human ileal microbiota. Environ. Microbiol. 12, 3213–3227.

Buffie, C.G., Jarchum, I., Equinda, M., Lipuma, L., Gobourne, A., Viale, A., et al., 2012. Profound alterations of intestinal microbiota following a single dose of clindamycin results in sustained susceptibility to *Clostridium difficile*-induced colitis. Infect. Immun. 80, 62–73.

Costerton, J.W., Lewandowski, Z., Caldwell, D.E., Korber, D.R., Lappin-Scott, H.M., 1995. Microbial biofilms. Annu. Rev. Microbiol. 49, 711–745.

Derrien, M., Vaughan, E.E., Plugge, C.M., de Vos, W.M., 2004. *Akkermansia muciniphila* gen. nov., sp. nov., a human intestinal mucin-degrading bacterium. Int. J. Syst. Evol. Microbiol. 54, 1469–1476.

Duarte, S., Cássio, F., Pascoal, C., 2012. Denaturing gradient gel electrophoresis (DGGE) in microbial ecology — insights from freshwaters. In: Magdeldin, S. (Ed.), Gel Electrophoresis — Principles and Basics. InTech, pp. 173–196.

Duncan, S.H., Scott, K.P., Ramsay, A.G., Harmsen, H.J., Welling, G.W., Stewart, C.S., et al., 2003. Effects of alternative dietary substrates on competition between human colonic bacteria in an anaerobic fermentor system. Appl. Environ. Microbiol. 69, 1136–1142.

Durban, A., Abellan, J.J., Jimenez-Hernandez, N., Ponce, M., Ponce, J., Sala, T., et al., 2011. Assessing gut microbial diversity from feces and rectal mucosa. Microb. Ecol. 61, 123–133.

Eckburg, P.B., Bik, E.M., Bernstein, C.N., Purdom, E., Dethlefsen, L., Sargent, M., et al., 2005. Diversity of the human intestinal microbial flora. Science 308, 1635–1638.

Ferrera, I., Sanchez, O., Mas, J., 2004. A new non-aerated illuminated packed-column reactor for the development of sulfide-oxidizing biofilms. Appl. Microbiol. Biotechnol. 64, 659–664.

Frank, D.N., St Amand, A.L., Feldman, R.A., Boedeker, E.C., Harpaz, N., Pace, N.R., 2007. Molecular-phylogenetic characterization of microbial community imbalances in human inflammatory bowel diseases. Proc. Natl. Acad. Sci. U. S. A. 104, 13780–13785.

Freter, R., Allweiss, B., O'Brien, P.C., Halstead, S.A., Macsai, M.S., 1981a. Role of chemotaxis in the association of motile bacteria with intestinal mucosa: in vitro studies. Infect. Immun. 34, 241–249.

Freter, R., O'Brien, P.C., Macsai, M.S., 1981b. Role of chemotaxis in the association of motile bacteria with intestinal mucosa: in vivo studies. Infect. Immun. 34, 234–240.

Fromin, N., Hamelin, J., Tarnawski, S., Roesti, D., Jourdain-Miserez, K., Forestier, N., et al., 2002. Statistical analysis of denaturing gel electrophoresis (DGE) fingerprinting patterns. Environ. Microbiol. 4, 634–643.

Gafan, G.P., Lucas, V.S., Roberts, G.J., Petrie, A., Wilson, M., Spratt, D.A., 2005. Statistical analyses of complex denaturing gradient gel electrophoresis profiles. J. Clin. Microbiol. 43, 3971–3978.

Gaskins, H.R., Croix, J.A., Nakamura, N., Nava, G.M., 2008. Impact of the intestinal microbiota on the development of mucosal defense. Clin. Infect. Dis. 46 (Suppl. 2), S80–6 (discussion S144-51).

Girvan, M.S., Campbell, C.D., Killham, K., Prosser, J.I., Glover, L.A., 2005. Bacterial diversity promotes community stability and functional resilience after perturbation. Environ. Microbiol. 7, 301–313.

Hong, P.Y., Croix, J.A., Greenberg, E., Gaskins, H.R., Mackie, R.I., 2011. Pyrosequencing-based analysis of the mucosal microbiota in healthy individuals reveals ubiquitous bacterial groups and micro-heterogeneity. PLoS ONE 6, e25042.

Jalanka-Tuovinen, J., Salonen, A., Nikkila, J., Immonen, O., Kekkonen, R., Lahti, L., et al., 2011. Intestinal microbiota in healthy adults: temporal analysis reveals individual and common core and relation to intestinal symptoms. PLoS ONE 6, e23035.

Jernberg, C., Lofmark, S., Edlund, C., Jansson, J.K., 2007. Long-term ecological impacts of antibiotic administration on the human intestinal microbiota. ISME J. 1, 56–66.

Kager, L., Liljeqvist, L., Malmborg, A.S., Nord, C.E., 1981. Effect of clindamycin prophylaxis on the colonic microflora in patients undergoing colorectal surgery. Antimicrob. Agents Chemother. 20, 736–740.

Lawley, T.D., Clare, S., Walker, A.W., Stares, M.D., Connor, T.R., Raisen, C., et al., 2012. Targeted restoration of the intestinal microbiota with a simple, defined bacteriotherapy resolves relapsing *Clostridium difficile* disease in mice. PLoS Pathog. 8, e1002995.

Macfarlane, S., Woodmansey, E.J., Macfarlane, G.T., 2005. Colonization of mucin by human intestinal bacteria and establishment of biofilm communities in a two-stage continuous culture system. Appl. Environ. Microbiol. 71, 7483–7492.

Magurran, A.E., 2004. Measuring Biological Diversity Measuring Biological Diversity. Blackwell Science Ltd., Malden, MA, USA.

Marzorati, M., Wittebolle, L., Boon, N., Daffonchio, D., Verstraete, W., 2008. How to get more out of molecular fingerprints: practical tools for microbial ecology. Environ. Microbiol. 10, 1571–1581.

McDonald, J.A., Schroeter, K., Fuentes, S., Heikamp-Dejong, I., Khursigara, C.M., de Vos, W.M., et al., 2013. Evaluation of microbial community reproducibility, stability and composition in a human distal gut chemostat model. J. Microbiol. Methods 95, 167–174.

Muyzer, G., de Waal, E.C., Uitterlinden, A.G., 1993. Profiling of complex microbial populations by denaturing gradient gel electrophoresis analysis of polymerase chain reaction-amplified genes coding for 16S rRNA. Appl. Environ. Microbiol. 59, 695–700.

Nyberg, S.D., Osterblad, M., Hakanen, A.J., Lofmark, S., Edlund, C., Huovinen, P., et al., 2007. Long-term antimicrobial resistance in *Escherichia coli* from human intestinal microbiota after administration of clindamycin. Scand. J. Infect. Dis. 39, 514–520.

Oteo, J., Aracil, B., Alos, J.I., Gomez-Garces, J.L., 2000. High prevalence of resistance to clindamycin in *Bacteroides fragilis* group isolates. J. Antimicrob. Chemother. 45, 691–693.

Peterfreund, G.L., Vandivier, L.E., Sinha, R., Marozsan, A.J., Olson, W.C., Zhu, J., et al., 2012. Succession in the gut microbiome following antibiotic and antibody therapies for *Clostridium difficile*. PLoS ONE 7, e46966.

Petrof, E.O., Claud, E.C., Gloor, G.B., Allen-Vercoe, E., 2013a. Microbial ecosystem therapeutics: a new paradigm in medicine? Benefic. Microbes 4, 53–65.

Petrof, E.O., Gloor, G.B., Vanner, S.J., Weese, J.S., Carter, D., Daigneault, M.C., et al., 2013b. Stool substitute transplant therapy for the eradication of *C. difficile* infection: RePOOPulating the gut. Microbiome 1, 1–12.

Pielou, E.C., 1975. Ecological Diversity Ecological Diversity. Wiley, New York.

Png, C.W., Linden, S.K., Gilshenan, K.S., Zoetendal, E.G., McSweeney, C.S., Sly, L.I., et al., 2010. Mucolytic bacteria with increased prevalence in IBD mucosa augment in vitro utilization of mucin by other bacteria. Am. J. Gastroenterol. 105, 2420–2428.

Possemiers, S., Verthe, K., Uyttendaele, S., Verstraete, W., 2004. PCR-DGGE-based quantification of stability of the microbial community in a simulator of the human intestinal microbial ecosystem. FEMS Microbiol. Ecol. 49, 495–507.

Probert, H.M., Gibson, G.R., 2004. Development of a fermentation system to model sessile bacterial populations in the human colon. Biofilms 1, 13–19.

Rajilic-Stojanovic, M., Heilig, H.G., Molenaar, D., Kajander, K., Surakka, A., Smidt, H., et al., 2009. Development and application of the human intestinal tract chip, a phylogenetic

microarray: analysis of universally conserved phylotypes in the abundant microbiota of young and elderly adults. Environ. Microbiol. 11, 1736–1751.
Reeves, A.E., Theriot, C.M., Bergin, I.L., Huffnagle, G.B., Schloss, P.D., Young, V.B., 2011. The interplay between microbiome dynamics and pathogen dynamics in a murine model of *Clostridium difficile* infection. Gut Microbes 2, 145–158.
Sanchez, O., Ferrera, I., Mas, J., 2008. Laboratory model systems for the study of microbial communities. In: Van Dijk, T. (Ed.), Microbial Ecology Research Trends. Nova Biomedical Books, New York, pp. 87–114.
Sekirov, I., Russell, S.L., Antunes, L.C., Finlay, B.B., 2010. Gut microbiota in health and disease. Physiol. Rev. 90, 859–904.
Shen, X.J., Rawls, J.F., Randall, T., Burcal, L., Mpande, C.N., Jenkins, N., et al., 2010. Molecular characterization of mucosal adherent bacteria and associations with colorectal adenomas. Gut Microbes 1, 138–147.
Shi, L., Ardehali, R., Caldwell, K., Valint, P., 2000. Mucin coating on polymeric material surfaces to suppress bacterial adhesion paper. Colloids Surf. B 17, 229–239.
Smith, C.J., 1985. Characterization of Bacteroides ovatus plasmid pBI136 and structure of its clindamycin resistance region. J. Bacteriol. 161, 1069–1073.
Smith, B., Wilson, J.B., 1996. A consumer's guide to evenness indices. Oikos 76, 70–82.
Sun, J., Zhou, T.T., Le, G.W., Shi, Y.H., 2010. Association of *Lactobacillus acidophilus* with mice Peyer's patches. Nutrition 26, 1008–1013.
Swidsinski, A., Dorffel, Y., Loening-Baucke, V., Theissig, F., Ruckert, J.C., Ismail, M., et al., 2011. Acute appendicitis is characterised by local invasion with *Fusobacterium nucleatum*/necrophorum. Gut 60, 34–40.
Tannock, G.W., Munro, K., Harmsen, H.J., Welling, G.W., Smart, J., Gopal, P.K., 2000. Analysis of the fecal microflora of human subjects consuming a probiotic product containing *Lactobacillus rhamnosus* DR20. Appl. Environ. Microbiol. 66, 2578–2588.
Van den Abbeele, P., Grootaert, C., Possemiers, S., Verstraete, W., Verbeken, K., Van de Wiele, T., 2009. In vitro model to study the modulation of the mucin-adhered bacterial community. Appl. Microbiol. Biotechnol. 83, 349–359.
Van den Abbeele, P., Grootaert, C., Marzorati, M., Possemiers, S., Verstraete, W., Gerard, P., et al., 2010. Microbial community development in a dynamic gut model is reproducible, colon region specific, and selective for Bacteroidetes and *Clostridium* cluster IX. Appl. Environ. Microbiol. 76, 5237–5246.
Van den Abbeele, P., Van de Wiele, T., Verstraete, W., Possemiers, S., 2011. The host selects mucosal and luminal associations of coevolved gut microorganisms: a novel concept. FEMS Microbiol. Rev. 35, 681–704.
Van den Abbeele, P., Belzer, C., Goossens, M., Kleerebezem, M., De Vos, W.M., Thas, O., et al., 2012a. Butyrate-producing *Clostridium* cluster XIVa species specifically colonize mucins in an in vitro gut model. ISME J. 7, 949–961.
Van den Abbeele, P., Roos, S., Eeckhaut, V., MacKenzie, D.A., Derde, M., Verstraete, W., et al., 2012b. Incorporating a mucosal environment in a dynamic gut model results in a more representative colonization by lactobacilli. Microb. Biotechnol. 5, 106–115.
Vermeiren, J., Van den Abbeele, P., Laukens, D., Vigsnaes, L.K., De Vos, M., Boon, N., et al., 2012. Decreased colonization of fecal *Clostridium coccoides/Eubacterium rectale* species from ulcerative colitis patients in an in vitro dynamic gut model with mucin environment. FEMS Microbiol. Ecol. 79, 685–696.
Wang, Y., Antonopoulos, D.A., Zhu, X., Harrell, L., Hanan, I., Alverdy, J.C., et al., 2010. Laser capture microdissection and metagenomic analysis of intact mucosa-associated microbial communities of human colon. Appl. Microbiol. Biotechnol. 88, 1333–1342.
Willing, B.P., Dicksved, J., Halfvarson, J., Andersson, A.F., Lucio, M., Zheng, Z., et al., 2010. A pyrosequencing study in twins shows that gastrointestinal microbial profiles vary with inflammatory bowel disease phenotypes. Gastroenterology 139, 1844–1854.e1.
Zoetendal, E.G., von Wright, A., Vilpponen-Salmela, T., Ben-Amor, K., Akkermans, A.D., de Vos, W.M., 2002. Mucosa-associated bacteria in the human gastrointestinal tract are uniformly distributed along the colon and differ from the community recovered from feces. Appl. Environ. Microbiol. 68, 3401–3407.